CHINESE OPTICS LETTERS

Vol. 21, No. 3 | March 2023

Highly efficient transient stimulated Raman scattering on secondary vibrational mode of $BaWO_4$ crystal due to its constructive interference with self-phase modulation

Igor Kinyaevskiy, Valeri Kovalev*, Pavel Danilov, Nikita Smirnov, Sergey Kudryashov, Andrey Koribut, and Andrey Ionin

P.N. Lebedev Physical Institute of the Russian Academy of Sciences, Moscow 119991, Russia

*Corresponding author: kovalevvi@lebedev.ru

Received September 16, 2022 | Accepted November 11, 2022 | Posted Online March 14, 2023

An exceptionally high stimulated Raman scattering (SRS) conversion efficiency to the first Stokes component associated with the secondary (low-frequency and low intensity) vibrational mode ν_2 ($\sim$330 cm^{-1}) was observed in a $BaWO_4$ crystal in a highly transient regime of interaction. The effect takes place in the range of pump pulse energy from $\sim$0.1 to $\sim$0.5 μJ with maximum energy conversion efficiency up to 35% at 0.2 μJ. The nature of the observed effects is explained by interference of SRS and self-phase modulation, where the latter is related to a noninstantaneous orientational Kerr nonlinearity in the $BaWO_4$ crystal.

Keywords: stimulated Raman scattering; secondary vibrational mode; self-phase modulation; ultrashort laser pulses; transient phenomena.

DOI: 10.3788/COL202321.031902

1. Introduction

Stimulated Raman scattering (SRS) remains one of the most popular and efficient techniques for conversion of laser radiation into spectral regions that are not accessible with traditional laser sources. As such, a search for media and schemes for SRS realization with various frequency shifts is actual and important. Conventionally, to realize a required radiation frequency via SRS, a medium with an appropriate Raman resonance frequency is searched for. While almost all SRS-active media are characterized by a range of Raman resonances[1,2], the strongest one only plays a role in a conventional single-pass scheme of SRS interaction[3]. A noticeable contribution of weaker ("secondary") Raman mode(s) to scattered radiation in Raman-active crystals was realized so far in schemes of a Raman laser with only a specially designed cavity[4–11]. Of these, the Stokes frequency shift associated with secondary Raman modes alone was reported for a self-Raman laser using Nd-doped Raman-active crystals[4–7]. In Raman laser using pure Raman-active crystals, the frequency shift corresponding to a weaker mode was only observed in combination with the stronger one(s)[8–10].

An appearance of notable SRS on the secondary Raman mode ν_2 alone in a conventional single-pass scheme of interaction may be found in Ref. [12]; however, emphasis there was given to the nature of asymmetric spectral broadening of pump radiation in $BaWO_4$ (BWO) crystal. Another unusual observation in Ref. [12] was (i) a low pump pulse energy for the ν_2 Raman mode spectral peak emerging, which was much lower than that for the strongest ν_1 Raman mode, and (ii) decay of that peak at higher pump pulse energy. In this Letter, we study these effects in detail, quantify them, and present a model explaining them.

2. Experiment and Results

The second-harmonic radiation ($\lambda = 515$ nm) of TEM_{00} laser beam generated by the ytterbium fiber oscillator/amplifier laser system Satsuma (Amplitude Systems) was used as pump radiation (Fig. 1). The system emitted pulses of 0.3 ps FWHM duration with energy E_p up to 3.4 μJ at 1 kHz pulse repetition rate. The beam was focused into the center of a BWO sample by a lens with the focal length of 35 mm. The focal waist FWHM diameter d_w and length l_w in the sample were 20 μm and 2.3 mm, respectively. The transmitted radiation was directed through a lens with the focal length of 100 mm into the spectrometer Avesta-150 FT. A neutral attenuator in front of the entrance slit prevented the spectrometer output saturation. The BWO crystal sample of nominally pure composition was grown at the Department of Laser Materials and Photonics of the General Physics Institute of the Russian Academy of Sciences. The sample of 8 mm length L was installed under normal incidence of the beam with the direction of the beam propagation k and, in contrast to the case in Ref. [13], polarization E was perpendicular to the BWO optical c axis.

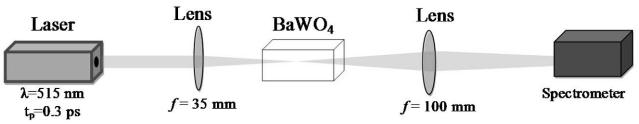

Fig. 1. Optics scheme of the experiment.

First, the spontaneous Raman scattering spectrum of our BWO sample was measured in the chosen configuration of interaction. The spectrum obtained with the Raman spectrometer Confotec 350-MR is presented in Fig. 2. It consists of the typical (for BWO) set of peaks[14] with the strongest peak at $\nu = 925\ \mathrm{cm}^{-1}$ (ν_1 mode), ~4.5 times lower height peak at ~330 cm^{-1} (ν_2 mode), ~6.5 times lower height peaks at ~800 cm^{-1} (ν_3 modes), and the set of much lower height peaks at $\nu = 60$–$180\ \mathrm{cm}^{-1}$ (ν_{ext} modes).

Afterwards, radiation spectra of 0.3 ps 515-nm laser pulses passing through the BWO sample were measured in several series with variable steps of E_p change. Figure 3 shows an example of the spectrum evolution with the E_p increase.

The spectra demonstrate a trend of broadening with the E_p increase, which is asymmetric with respect to Stokes and anti-Stokes wings, as in Ref. [12]. On such a background, the first pronounced peak appears at $\lambda \approx 524$ nm (corresponding to the ν_2 secondary Raman mode) at E_p between 0.1 μJ and 0.12 μJ, i.e., well before the peak appearing at $\lambda \approx 540$ nm corresponding to SRS on the about 5 times stronger ν_1 mode (see Fig. 2). The spectra corresponding to $E_p \approx 0.12$ and 0.19 μJ in Fig. 3 show that conversion to the scattered signal was high enough for an essential depletion of the pump. The amplitude of the 524 nm peak remains high up to $E_p \approx 0.3$–0.4 μJ and decreases down to the background level at $E_p > 0.5$ μJ. The peak at $\lambda \approx 540$ nm then appears at $E_p \approx 1.3$ μJ only. With further increase of E_p, the amplitude of this peak grows up to its maximum at $E_p \approx 1.8$ μJ and then goes down. No pronounced peaks corresponding to SRS on ν_3 Raman modes were observed in all the sets of measurements. All these features look very similar to those observed in Refs. [12,13] for SRS on ν_1 mode. Except for decay of the peaks with increase of E_p, these features were accounted for as a result of seeding SRS by the pump spectrally broadened via self phase modulation (SPM).

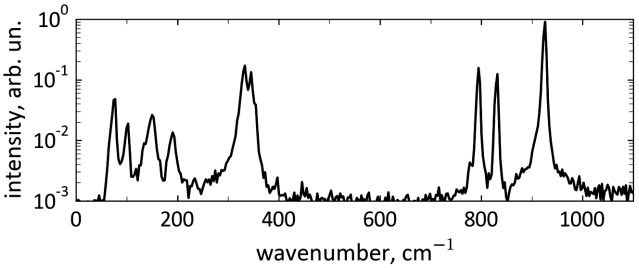

Fig. 2. Spontaneous Raman spectrum of the BWO crystal when k and E are perpendicular to the c axis.

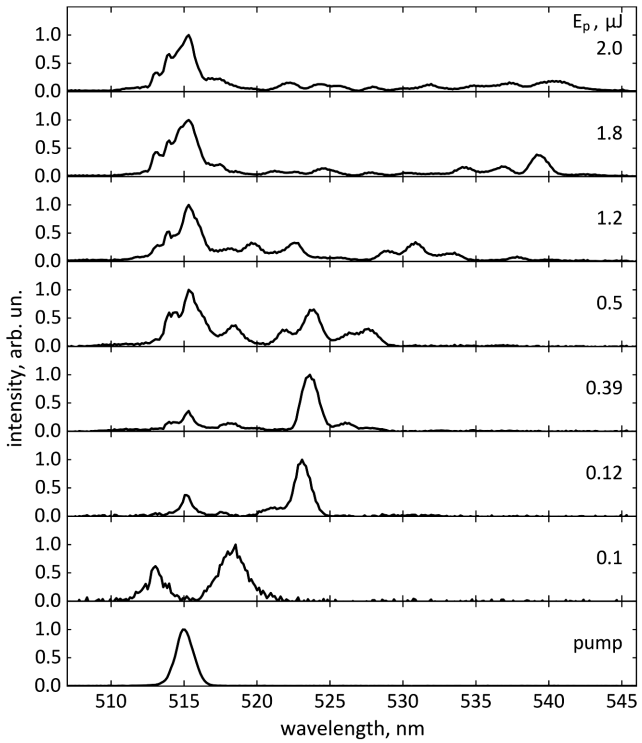

Fig. 3. Spectra of passing through BWO radiation at different E_p.

Two techniques were used for examination of the conversion efficiency K of SRS on the ν_2 mode. In the first one, the dependence of K on E_p is obtained from the spectra, examples of which are presented in Fig. 3, as the ratio of area under the peaks to the area under whole transmitted/output spectrum at the correspondent E_p. Figure 4 shows the dependence of the relative value of K on E_p for the peak at 524 nm for three series of measurements with the other invariant conditions. While fluctuating from series to series, the data show the trend of a rapid increase of K at $E_p \geq 0.1$ μJ, attaining a maximum at $E_p \approx 0.2$–0.3 μJ and lowering to a background level at $E_p > 0.5$ μJ. The dashed curve in Fig. 4 is an interpolation of $K(E_p)$ after averaging magnitudes of K at each E_p.

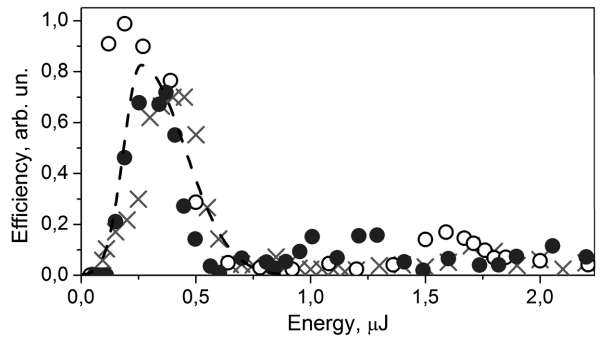

Fig. 4. Dependence of SRS efficiency K at ν_2 BWO Raman mode on pump pulse energy E_p. Different symbols correspond to different experimental series.

The data in Fig. 4 are given in relative units because the method of obtaining K that was used does not allow one to adequately account for an effect of a difference in spatial distributions of the transmitted pump and generated copropagating Stokes radiation. To avoid the effect and evaluate the absolute values of K, we used the technique in which the transmitted radiation was sent to an energy meter (Ophir PD10-C) through a 1200 gr/mm grating that separated pump and Stokes beams. An aperture in front of the energy meter allowed passing the Stokes radiation beam up to the level ≥ 0.1 of maximum. In such a configuration, a contribution to the measured energy from the broadened pump was less than 2%, and the Stokes radiation energy underrating was 10%. As a consequence, the accuracy of defining K was evaluated as ~12%. The system was calibrated at $E_p \approx 0.05$ μJ. The K on E_p dependence was similar to that shown by the dashed line in Fig. 4; at $E_p \approx 0.3$ μJ, the absolute value of K peaked 35% with the average magnitude 30% ± 5%. These high magnitudes are the record ones, if compared to all results published up to now on SRS involving secondary Raman modes[4–11]. This efficiency is much higher than that for the strongest ν_1 (925 cm^{-1}) Raman mode (by ~2.3 times following from the data in the present work and by ~1.5 times that in Ref. [13]). A reason for this is clear from the spectra for $E_p = 1.8$ μJ: a much higher part of the incident pump energy is transformed into the SPM-broadened radiation, which does not contribute to seeding the SRS on the ν_1 Raman mode.

Based on the presented above results and gained knowledge in Refs. [12,13], we propose the following scenario for the information presented above and observed earlier in Refs. [12,13] experimental data. Figure 5 illustrates this scenario. The incident pump pulse is presumed to be Gaussian with FWHM duration $t_p = 0.3$ ps [see diagram (A)]. Propagating through the BWO sample, this pulse experiences spectral broadening due to SPM. Curves 1–4 in diagram (B) show the dynamics of the SPM-induced wavenumber deviation $\Delta\nu = \Delta\nu_{tr}(t, E_p)$ in BWO at four different levels of E_p. The curves are calculated using the equation[12],

$$\Delta\nu_{tr}(t, E_p) = \frac{n^2 n_2}{t_p \tau_{NL} \lambda^2 c} E_p \int_{-\infty}^{t} e^{-(1.67x/t_p)^2} e^{-(t-x)/\tau_{NL}} dx \, [\mathrm{cm}^{-1}], \quad (1)$$

which accounts for the transient character of SPM in the conditions of our experiments. In Eq. (1), $n = 1.85$ is the linear refractive index, $n_2 = 6.3 \times 10^{-15}$ cm^2/W is the nonlinear refractive index of BWO[12,15], which is responsible for SPM, $\tau_{NL} = 0.35$ ps is its decay time, λ is the pump radiation wavelength, and c is the speed of light in vacuum. Diagram (C) in Fig. 5 mimics the presented in the Fig. 2 spectrum of spontaneous Raman scattering of BWO when k and E are perpendicular to the c axis of the crystal.

First, the data in diagram (B) show that the broadening to the anti-Stokes side is less than that to the Stokes side, which is consistent with observed asymmetry of the spectra. Second, the anti-Stokes SRS components were observed neither in this work, nor

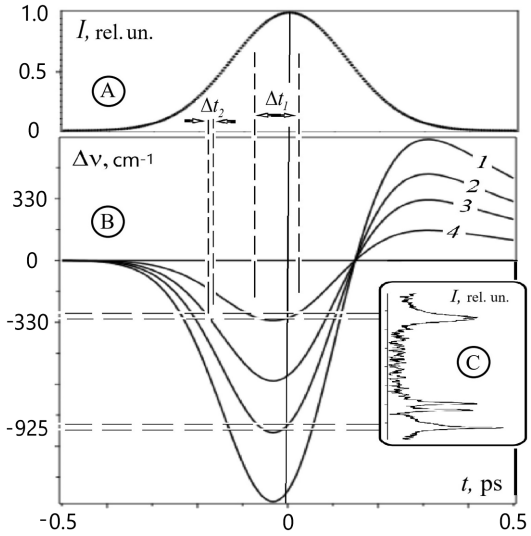

Fig. 5. The exemplification of spectral-temporal matching of SPM and SRS in BWO. Diagram (A), pump pulse; diagram (B), dynamics of spectral broadening due to SPM (chirp) at different E_p (curves 1–4); diagram (C), BWO spontaneous Raman scattering spectrum.

in Refs. [12,13] because a deviation $\Delta\nu$ to the anti-Stokes side ($\Delta\nu > 0$) exists at the trailing part of the pump pulse. Regarding the Stokes side ($\Delta\nu < 0$), when the amplitude of $\Delta\nu$ is about the wavenumber of Raman modes ν_2 & ν_1 (curves 1 and 3), the intensity of incident pump pulse is near its maximum and time Δt_1 for interaction of the corresponding seeding signal with the pump pulse (the distance between the vertical dashed lines) is the longest. This provides the best conditions for the SRS amplification of the corresponding Raman mode, and the E_p at which this effect takes place may be called an optimal one. In such a model, modes ν_3 do not emerge, most probably, because they are overtaken by the much stronger mode ν_1.

When E_p is below the optimal one, $\Delta\nu$ is notably lower than the wavenumber of the corresponding Raman mode (ν_1 or ν_2), and the power and intensity of the seeding and pump signals are lower than those required for SRS-caused amplification of the corresponding Raman component to a measurable magnitude (sometimes attributed to the SRS threshold). When E_p is higher than the optimal one for excitation of the Raman mode (curves 2 and 4 for modes ν_2 and ν_1, respectively), $\Delta\nu$ required for optimal seeding either the ν_1 or ν_2 mode takes place at the leading and trailing edges of the pump pulse (A), i.e., not at the maximum of the pump pulse. In this case, the time interval Δt_2, during which the seeding radiation is "in the resonance" with the Raman mode, is shorter than that at the optimal E_p. Both these circumstances result in worsening the conditions for SRS amplification of corresponding modes, and, consequently, one would expect their disappearance in registered spectra. In reality/practice, however, already excited Raman components exist in the spectra for some extended ranges of E_p: from ~0.12 μJ to ~0.5 μJ for the ν_2 mode and from ~1.3 μJ to ~2 μJ for the ν_1 mode (see Fig. 3). The effect responsible for this fact was noted in our earlier

paper[12]—a saturation of the SPM-induced broadening rate when conversion of the pump energy to a Raman mode is high (see Fig. 3 in Ref. [12]).

To illustrate the seed effect of SPM, the SPM-broadened spectra for our experiment are calculated using Eq. (1) and corresponding parameters of BWO, and are presented in Fig. 6 by dashed lines. Experimental spectra (mimicked from Fig. 3) are presented in Fig. 6 by solid lines. The vertical line marks the position of wavelength $\lambda = 524$ nm that corresponds to the conventional SRS[16] on the ν_2 Raman mode of BWO.

At $E_p = 0.1$ μJ, both spectra demonstrate a reasonable correspondence, at least for the Stokes side, and absence of a notable spectral peak above the background noise level (the amplitude of ~3% of the pump intensity in our system) at ~524 nm. The coincidence disappears with an increase of E_p up to 0.12 μJ. While for $E_p = 0.12$ μJ, the calculated spectrum demonstrates only a slight change, the experimental one changes radically: a strong peak at about 524 nm appears. At this level of pump, the relative K, being on an average ~0.5, fluctuates from ~0.2 up to ~0.9 of the peak value (see Fig. 4), and the peak maximum appears shifted to a shorter λ, from 524 nm to ~523 nm.

A comparison of the results at $E_p = 0.1$ μJ and 0.12 μJ shows that a slight, 20%, growth of E_p must provide a proper increase of both the seeding signal amplitude and the SRS amplification. Corresponding calculations of the long wavelength tail of the SPM-broadened pump spectrum demonstrated a tenfold increase of the seeding signal amplitude at $\lambda = 524$ nm only. Afterwards, we evaluated the contribution of the SRS amplification presuming an exponential growth of a seeding signal. The amplification is described as $G = \exp(g_{R2} I_p l)$, where $I_p = 4E_p/\pi d_w^2 t_p$ is the pump radiation intensity, l is the SRS interaction length, and g_{R2} is the SRS gain coefficient on the ν_2 mode. The latter is the only unknown parameter in this expression. Its magnitude in our experimental conditions is evaluated as $g_{R2} \cong g_{R1}(T_2/T_1)(t_p/T_2)/4.5$, where g_{R1} is the steady state SRS gain coefficient on the ν_1 mode, the ratio (T_2/T_1) accounts for the effect of difference in decay time $T_{1,2}$ of modes $\nu_{1,2}$[3,16], the ratio (t_p/T_2) accounts for the transient character of SRS[16], and the factor "4.5" is the ratio of the ν_1 and ν_2 peak heights (see Fig. 2). By using the known parameters of BWO (g_{R1}= 40 cm/GW at 515 nm, $T_1 = 6.6$ ps, and $T_2 = 3$ ps[3,9]) one would get $g_{R2} = 0.4$ cm/GW. Then, presuming $l = l_w = 0.23$ cm, the increase of SRS amplification is $\Delta G \approx 6$ with an increase of pump pulse energy E_p from 0.1 to 0.12 μJ. This fact, together with the tenfold increase of seeding signal intensity, is consistent with the experimental observations. According to these estimates, even minute possible fluctuations of E_p in our case may be a reason for the observed big fluctuations of K at 0.12 μJ.

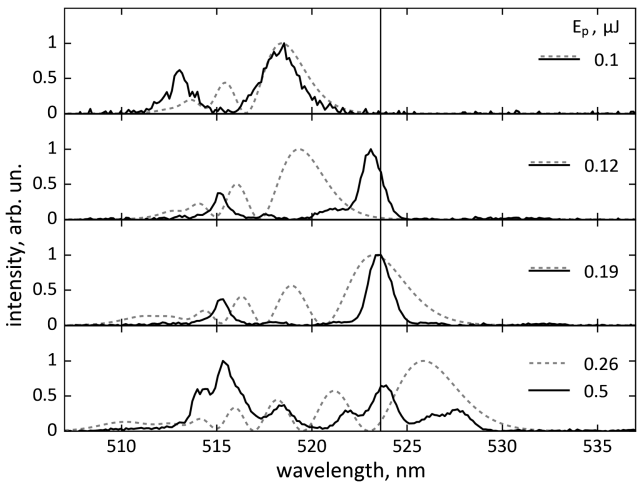

Fig. 6. Calculated spectra of SPM broadened in BWO laser pulse (dashed lines) and experimental spectra (solid lines) at different E_p.

At $E_p = 0.19$ μJ, the maxima of the calculated spectrum and experimental peak coincide at 524 nm, and K increases to 30% ± 5%. At $E_p = 0.19$ μJ, the maximum of the SPM-broadened spectrum exactly matches the Raman shift, which is the best-case scenario, providing the highest SRS conversion efficiency (Fig. 4). At $E_p = 0.5$ μJ, the maximum of SPM-broadened spectrum according to Eq. (1) should be far away from the ν_2 SRS resonance. In reality, however, this does not happen, because of the effect of SPM broadening reduction when the SRS conversion efficiency is high[12]. That is the reason why the calculated SPM broadening with $E_p = 0.26$ μJ most closely corresponds to the experimental spectrum at $E_p = 0.5$ μJ.

In contrast to the case at $E_p = 0.12$ μJ, at $E_p = 0.5$ μJ, the peak's wavelength shifted from 524 nm to a longer λ (~524.2 nm). In both cases, the observed shifts are a consequence of the frequency pulling phenomenon[17].

3. Conclusion

An incredibly high SRS conversion efficiency (energy efficiency up to 35%) is for the first time obtained on a low-frequency secondary ν_2(330 cm^{-1}) Raman mode in a BWO crystal pumped by 0.3 ps 515 nm wavelength laser pulses in a simple single-pass scheme of SRS interaction. This result is interpreted as a consequence of constructive interference of the transient SRS and SPM effects when correspondent Raman Stokes component is seeded by SPM-caused spectral broadening of the pump radiation, which is asymmetric in the BWO crystal because of its non-instantaneous orientational Kerr nonlinearity. The obtained results confirm and extend the model of transient SRS and SPM in a BWO crystal proposed in Refs. [12,13]. While the effects discussed above observed in the BWO crystal and their theoretical models are developed, these actually are not sample-specific. Therefore, these would work in other SRS-active crystals[1] to a varying degree. The practical significance of these results is a possibility of extending the range of frequencies generated by all-solid laser systems with high energy efficiency and the possibility of their control by varying the pump pulse energy.

Acknowledgement

We are grateful to Dr. Elizaveta Dunaeva of A. M. Prokhorov General Physics Institute of the Russian Academy of Sciences

for providing the $BaWO_4$ crystal. This research was funded by the Russian Science Foundation (No. 22-79-10068).

References

1. T. T. Basiev, A. A. Sobol, P. G. Zverev, L. I. Ivleva, V. V. Osiko, and R. C. Powell, "Raman spectroscopy of crystals for stimulated Raman scattering," Opt. Mater. **11**, 307 (1999).
2. http://rruff.info.
3. P. Cherny, H. Jelınkova, P. G. Zverev, and T. T. Basiev, "Solid state lasers with Raman frequency conversion," Progr. Quantum Electron. **28**, 113 (2004).
4. J. Lin and H. M. Pask, "Cascaded self-Raman lasers based on 382 cm^{-1} shift in Nd:$GdVO_4$," Opt. Express **20**, 15180 (2012).
5. R. Li, R. Bauer, and W. Lubeigt, "Continuous-wave Nd:YVO_4 self-Raman lasers operating at 1109 nm, 1158 nm and 1231 nm," Opt. Express **21**, 17745 (2013).
6. F. Bai, Z. Y. Jiao, X. F. Xu, and Q. P. Wang, "High power Stokes generation based on a secondary Raman shift of 259 cm^{-1} of Nd:YVO_4 self-Raman crystal," Opt. Laser Technol. **109**, 55 (2019).
7. S. Li, R. Tang, G. Jin, and C. Wang, "Actively *Q*-switched intracavity Nd:YVO_4/$GdVO_4$ Raman laser operating with multiple Raman shifts of 259, 882 and 890 cm^{-1},"Appl. Phys. B **127**, 16 (2021).
8. P. G. Zverev, T. T. Basiev, A. A. Sobol, I. V. Ermakov, and W. Gellerman, "$BaWO_4$ crystal for quasi-cw yellow Raman laser," in *Advanced Solid-State Lasers*, C. Marshall, ed., Vol. **50** of OSA Trends in Optics and Photonics (Optica Publishing Group, 2001), paper ME1.
9. M. Frank, S. N. Smetanin, M. Jelínek, D. Vyhlídal, L. I. Ivleva, P. G. Zverev, and V. Kubeček, "Highly efficient picosecond all-solid-state Raman laser at 1179 and 1227 nm on single and combined Raman lines in a $BaWO_4$ crystal," Opt. Lett. **43**, 2527 (2018).
10. M. Frank, S. N. Smetanin, M. Jelínek, D. Vyhlídal, K. A. Gubina, V. E. Shukshin, P. G. Zverev, and V. Kubecek, "Multiwavelength, picosecond, synchronously pumped, $Pb(MoO_4)_{0.2}(WO_4)_{0.8}$ Raman laser oscillating at 12 wavelengths in a range of 1128–1360 nm," Opt. Lett. **46**, 5272 (2021).
11. V. S. Gorelik and A. V. Skrabatun, "Stimulated multifrequency Raman scattering of light in a polycrystalline sodium bromate powder," Spectrochim. Acta A **245**, 118889 (2021).
12. I. O. Kinyaevskiy, V. I. Kovalev, P. A. Danilov, N. A. Smirnov, S. I. Kudryashov, A. V. Koribut, and A. A. Ionin, "Asymmetric spectral broadening of sub-picosecond laser pulse in $BaWO_4$ crystal: interplay of self-phase modulation, stimulated Raman scattering, and orientational Kerr nonlinearity," Opt. Lett. **46**, 697 (2021).
13. I. O. Kinyaevskiy, V. I. Kovalev, P. A. Danilov, N. A. Smirnov, S. I. Kudryashov, L. V. Seleznev, E. E. Dunaeva, and A. A. Ionin, "Highly efficient stimulated Raman scattering of sub-picosecond laser pulses in $BaWO_4$ for 10.6 μm difference frequency generation," Opt. Lett. **45**, 2160 (2020).
14. T. T. Basiev, A. A. Sobol, Y. K. Voronko, and P. G. Zverev, "Spontaneous Raman spectroscopy of tungstate and molybdate crystals for Raman lasers," Opt. Mater. **15**, 205 (2000).
15. I. O. Kinyaevskiy, V. I. Kovalev, A. V. Koribut, P. A. Danilov, N. A. Smirnov, S. I. Kudryashov, Y. V. Grudtsyn, E. E. Dunaeva, V. A. Trofimov, and A. A. Ionin, "Asymmetric spectral broadening of 0.3 ps 1030 nm laser pulse in $BaWO_4$ crystal," J. Russ. Laser Res. **43**, 315 (2022).
16. R. W. Boyd, *Nonlinear Optics*, 3rd ed. (Academic, 2007).
17. O. Svelto and D. C. Hanna, *Principles of Lasers*, 4th ed. (Plenum, 1998).